

CHAPTER - II

PREPARATION AND CHARACTERIZATION



CHAPTER - II

Part - A

2.A.1 Introduction

The properties of ferrites are both intrinsic as well as structure sensitive. The extrinsic properties can be controlled with the help of the control over the preparation technique. The porosity, impurity and grain size mostly affect the extrinsic properties of ferrites. The purity, chemical homogeneity, stoichiometry, grain size etc. also need to be controlled while preparing the ferrites. In this section the general methods of ferrite preparation are discussed briefly.

2.A.2 Methods of Ferrite Preparation

The ferrites are oxide ceramics and could be formed very easily by the ceramic method. The ferrite fabrication technique generally involves the following steps -

- 1) preparation of ferrites having desired chemical formula
- 2) compacting the ferrite powder in desired shape
- 3) sintering the compact at high temperature to get the final product

2.A.3 Preparation of Ferrite Composition

The four general methods of preparing ferrite composition are in practice and are as follows -

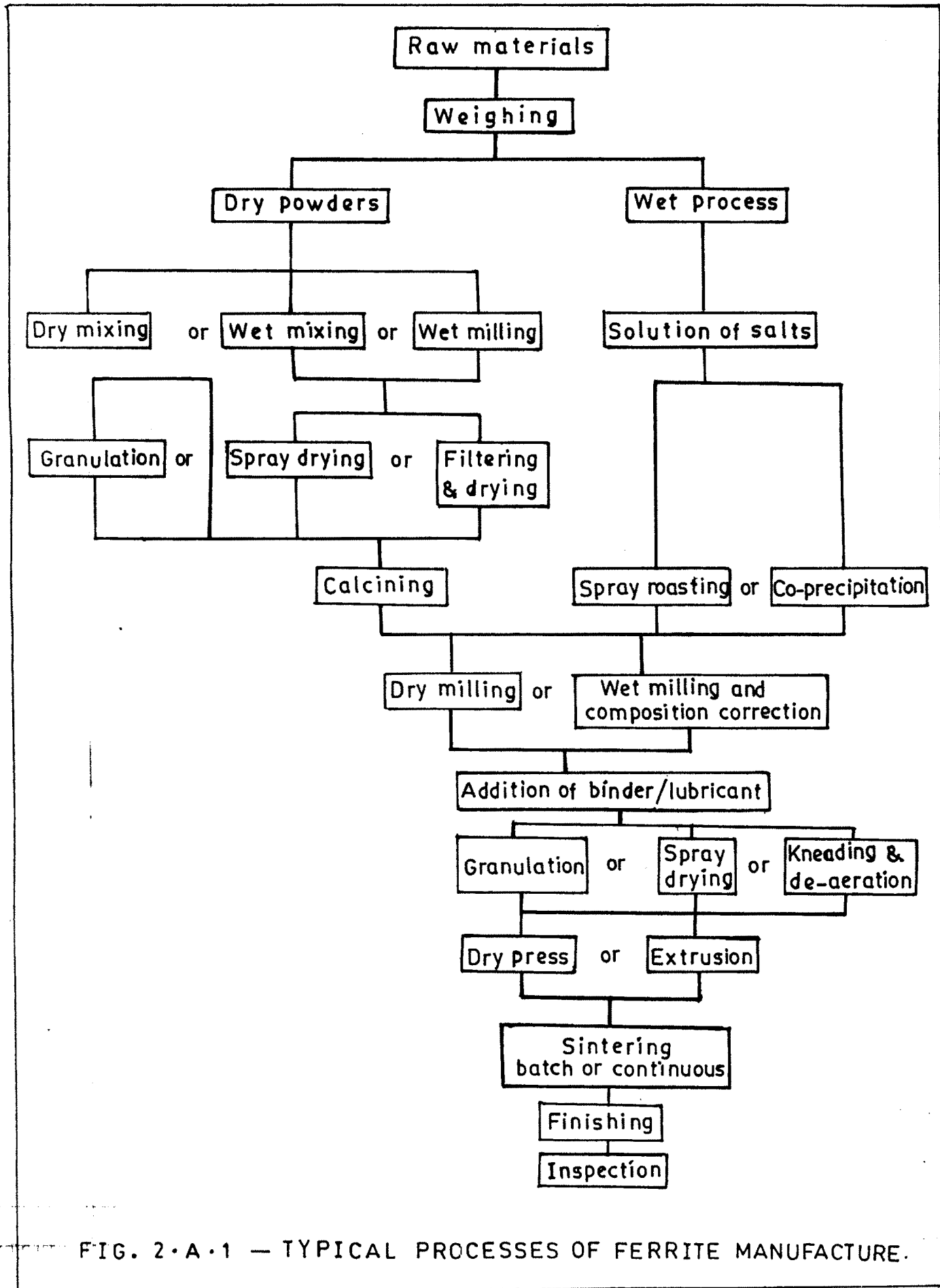


FIG. 2·A·1 — TYPICAL PROCESSES OF FERRITE MANUFACTURE.

a) Ceramic method

In this method high purity divalent metal oxides are physically mixed with iron oxide using the ball mill. The mixture is presintered at a suitable temperature for suitable duration. It is furnace cooled, mechanically powdered and sieved to avoid the large sized particles. The powder is pressed in the die to obtain required shape and subjected to final sintering at high temperatures. The method is comparatively simpler, gives good results and requires little chemical knowledge.

b) Decomposition method

Instead of using oxides as starting materials, in this method the salts such as carbonates, nitrates and oxalates are used. These compounds are weighed for mixing and preheated usually in air which produces their oxides by thermal decomposition. The oxides which are prepared by decomposition more rapidly undergo solid state reaction.¹ Other details of this method are similar to ceramic method.

c) Hydroxide precipitation method

The hydroxides are precipitated simultaneously from a solution so that precipitate contains the required metal ions in the correct proportions. Economus² established this method for ferrite preparation. Recently Robbins³ prepared manganese zinc ferrite by chemical co-precipitation with hydroxide and

carbonate. The hydroxide precipitation method is also applied for the preparation of yttrium iron garnet by Wolf et al⁴. The qualitative understanding of chemical process involved is essential, because the simultaneous precipitation hydroxides has to be complete. Sato et al^{5,6} prepared ultrathin spinel ferrites by this method.

d) Oxalate Precipitation Method

Due to some reasons, precipitation of metallic oxalates is necessary. The precipitation can be carried out by using ammonium oxalate which does not leave any residue after heating. Due to similar crystal structure of most oxalates they can be readily precipitated after adding ammonium oxalates to their salt solutions. Here also the mixing in correct ratios can be affected upto molecular scale. However, the precipitation rate does not differ widely. After careful heating, the oxalates get thermally decomposed which gives water and di-oxide. After careful calcination at temperature of precipitation, it yields ferrites with particle size less than 1 micron. Lin Bo Zhas⁷ prepared Mn-Zn ferrites by this method.

2.A.4 Solid State Reaction

In ceramic method, the solid state reaction plays an important role in the formation of spinel ferrites and it can be discussed on the basis of diffusion of components involving

divalent metal oxide and Fe_2O_3 . In the initial configuration there is only one phase boundary between reactants. After the nucleation of ferrites, the boundary is replaced by different phase boundaries, one between Mo and MFe_2O_4 and other between Fe_2O_3 and MFe_2O_4 . In this state further progress of the reaction can only take place by transport of reactants through the ferrite phase. There are three possible mechanisms. In counter diffusion mechanism suggested by Wagner⁶ only cations migrate in the opposite directions, the oxygen ions are essentially stationary. In the second mechanism the anions take part in the diffusion process. In this reaction diffusion of one cation is compensated by an associated flux of anions (O^{2+}) instead of a counter current of another cation. In third mechanism iron is diffused through the ferrite layer in the reduced state i.e. Fe^{2+} . In such a case oxygen is transported through the gas phase, being given off at $\text{MFe}_2\text{O}_4/\text{Fe}_2\text{O}_3$ interface and taken up again at $\text{Mo}/\text{Fe}_2\text{O}_4$ boundary.

2.A.5 Preparation of ferrite samples (Present case)

The ceramic technique involving double sintering is used in the present case. In the ferrite system $\text{Mg}_x\text{Cd}_{1-x}\text{Sm}_y\text{Fe}_{2-y}\text{O}_4$ six samples with $x = 0.5$ and $y = 0, 0.1, 0.2, 0.3, 0.4$ and 0.5 were prepared. High purity oxides of magnesium, cadmium, samarium and iron were weighed in desired proportion and mixed physically

in agate mortar in acetone medium. The presintering was carried out at 800°C for 12 hours. The samples were furnace cooled and pressed in the form of pellets (1 cm diameter) and toroids (ID = 1cm and OD = 1.5 cm) using a hydraulic press. The pellets were finally sintered for 1000°C for 40 hrs. The physical densities were calculated with help of weight and dimension data.

Part - B

Characterization by X-ray diffraction

2.B.1 Introduction

X-rays are diffracted by the solids. With the help of x-ray diffraction one can determine (i) the crystallinity of a given solid and its crystal structure, (ii) evaluate the nature of the phases present (iii) calculate structural parameters and (iv) study the crystal imperfections. X-ray diffraction plays an important role in ferrite research.

According to Bragg's law X-rays get diffracted from a plane (hkl) when the equation

$$2d (hkl) \sin \theta = n\lambda \quad \dots (2.B.1)$$

where n - order of reflection

d - interplaner distance for plane (hkl)

and θ - glancing angle. is satisfied.

Similar to X-rays, electrons and neutrons are also employed in determining the crystal structure of ferrites. The scattering power of the thermal neutrons is partly determined by the magnetic moment of the nucleus of the atoms, due to interaction with the electron spin. This always varies considerably for atoms having roughly the same number of electrons, so that neutron diffraction is able to provide an information on the occupation of the two spinel sites by ions of the transition elements. The penetrating power of neutron is very high. If the elements differ by only one atomic number, neutron diffraction can show well distinguished lines. The atoms of ferrites have a net magnetic moment which interacts with the neutron magnetic moment. The neutron diffraction study for ferrites is carried out by number of workers^{8,9,10}.

In the present study X-ray diffraction is used to (i) confirm the completion of solid state reaction (ii) observe impurity phases (iii) determine the lattice constant, interplaner distances, octahedral and tetrahedral site radii and bond lengths etc.

2.B.2 Diffraction of X-rays

X-ray diffraction technique is the well established techniques for the study of crystal structure of materials. It has been used both for the confirmation of the spinel phase

formation and to determine the lattice parameters in case of ferrites.

The simplest explanation of the observed diffraction maxima when X-ray radiation passes through the crystal was first given by Bragg¹². The diffraction maxima occur when Bragg law, viz. $2d \sin\theta = n\lambda$ is satisfied. The diffraction methods for crystal structure evaluation are available depending upon whether the θ (diffraction angle) or the λ (wavelength of X-rays) is varied. For all powder diffraction work the wavelength of the X-rays is kept constant and the sample is rotated in order to vary the Bragg angle. The method is popularly known as the powder method and used in the present case.

The powder method was developed by Debye and Scherrer¹³ and independently by Hull¹⁴. In this method a small quantity of smoothly ground powder is coated on a fine glass capillary with the help of a glue. The specimen is mounted on the movable mount provided at the center of Debye Scherrer camera with proper alignment. Since the fine grains of the powder sample are randomly oriented, the reciprocal lattice vectors of all the crystallites are pointed in all possible directions. The incident monochromatic X-ray radiation finds some crystal planes which satisfy the Bragg diffraction condition to produce the maxima. Since the diffracted X-rays from a particular set of plane lie along the surface of a cone with an apex angle 2θ , when they

intercept the film, produce a concentric ring. The cones coming from different set of planes similarly produce different concentric rings on the films. To ensure that all possible sets of planes face the incident monochromatic beam the sample is rotated with the help of an electric motor. In an XRD machine a counter is used instead of a film and direct graphical record of intensities of diffracted maxima as a function of 2θ is obtained.

2.B.3 X-ray diffraction methods

It was shown by Bragg that diffraction maxima occur when the Bragg's law,

$$2d \sin\theta = n\lambda \quad \dots (2.1)$$

where n = order of diffraction

λ = wavelength of X-rays

and d = interplaner distance is satisfied.

If (h,k,l) are the miller indices for a set of parallel planes, for cubic system the interplaner distance is given by,

$$d = a / \sqrt{h^2+k^2+l^2} \quad \dots (2.2)$$

from equation 1 and 2 we get for lattice parameter

$$a = n\lambda (h^2+k^2+l^2)^{1/2} / 2 \sin \theta \quad \dots (2.3)$$

monochromatic X-rays of wavelength λ striking a 3-dimensional crystal at an arbitrary angle incidence will not in general be

reflected. To satisfy Bragg's condition and to cause diffraction we have to vary either wavelength or glancing angle (θ). There are two other methods of crystal analysis by X-rays.

1) Laue Method

In this method a crystal is kept stationary in a beam of continuous X-rays. The crystal selects a suitable wavelength (λ) and diffraction occurs from a plane with incident glancing angle (θ).

2) Rotation Crystal Method

In this method a crystal is rotated about a fixed axis in a beam of X-ray having fixed wavelength. For particular θ Bragg's law is satisfied and diffraction occurs.

2.B.4 Results and Discussion

X-ray diffractogram of the samples $Mg_x Cd_{1-x} Sm_y Fe_{1-y} O_4$ ($x=0.5$ and $y=0, 0.1, 0.2, 0.3, 0.4, 0.5$) were obtained by using the computerized XRD unit (Philips model APD.1710) with $CuK\alpha$ radiation ($\lambda = 1.5418 \text{ \AA}$) at USIC, Shivaji University, Kolhapur. The lattice parameters and interplaner distances were calculated from X-ray diffractograms by using the standard formulae for the cubic system. The data on lattice parameters is given in Table 2.B.2 to 2.B.6 and that on density and porosity in Table 2.B.7. The diffraction maxima have been indexed in the light of the crystalstructure of natural spinel, $MgAl_2O_4$. The allowed

Table - 2.B.1

X-ray diffraction data for $\text{Mg}_{0.5}\text{Cd}_{0.5}\text{Sm}_0\text{Fe}_2\text{O}_4$ Wavelength $\lambda = 1.5418 \text{ \AA}$ Lattice parameter $a = 8.641 \text{ \AA}$

Structure = Cubic

Sr.No.	2θ deg.	$d_{\text{cal}} \text{ \AA}$	$d_{\text{obs}} \text{ \AA}$	(hkl)
1.	29.235	3.0523	3.056	220
2.	39.485	2.5987	2.605	311
3.	35.420	2.5322	2.495	222
4.	52.075	1.7548	1.764	422
5.	55.480	1.6549	1.662	333
6.	63.815	1.4574	1.528	440

Table - 2.B.2

X-ray diffraction data for $\text{Mg}_{0.5}\text{Cd}_{0.5}\text{Sm}_{0.1}\text{Fe}_{1.9}\text{O}_4$ Wavelength $\lambda = 1.5418 \text{ \AA}$ Lattice parameter $a = 8.6515 \text{ \AA}$

Structure = Cubic

Sr.No.	2θ deg.	$d_{\text{cal}} \text{ \AA}$	$d_{\text{obs}} \text{ \AA}$	(hkl)
1.	29.115	3.0611	3.0646	220
2.	34.325	2.6105	2.6105	311
3.	55.080	1.6660	1.6662	333
4.	60.705	1.5305	1.5244	440

Table - 2.B.3

X-ray diffraction data for $\text{Mg}_{0.5}\text{Cd}_{0.5}\text{Sm}_{0.2}\text{Fe}_{1.8}\text{O}_4$

Wavelength $\lambda = 1.5418 \text{ \AA}$

Lattice parameter $a = 8.6714 \text{ \AA}$

Structure = Cubic

Sr.No.	2θ deg.	$d_{\text{cal}} \text{ \AA}$	$d_{\text{obs}} \text{ \AA}$	(hkl)
1.	29.105	3.0667	3.0657	220
2.	34.260	2.6153	2.6153	311
3.	55.020	1.6693	1.6677	333
4.	60.305	1.5333	1.5335	440

Table - 2.B.4

X-ray diffraction data for $\text{Mg}_{0.5}\text{Cd}_{0.5}\text{Sm}_{0.3}\text{Fe}_{1.7}\text{O}_4$

Wavelength $\lambda = 1.5418 \text{ \AA}$

Lattice parameter $a = 8.6539 \text{ \AA}$

Structure = Cubic

Sr.No.	2θ deg.	$d_{\text{cal}} \text{ \AA}$	$d_{\text{obs}} \text{ \AA}$	(hkl)
1.	29.185	3.0618	3.0574	220
2.	34.315	2.6112	2.6112	311

Table - 2.B.5
X-ray diffraction data for $\text{Mg}_{0.5}\text{Cd}_{0.5}\text{Sm}_{0.4}\text{Fe}_{1.6}\text{O}_4$

Wavelength $\lambda = 1.5418 \text{ \AA}$

Lattice parameter $a = 8.7355 \text{ \AA}$

Structure = Cubic

Sr.No.	2θ deg.	$d_{\text{cal}} \text{ \AA}$	$d_{\text{obs}} \text{ \AA}$	(hkl)
1.	29.035	3.0766	3.0729	220
2.	34.145	2.6238	2.6238	311
3.	54.825	2.1755	2.6731	400
4.	58.960	1.5383	1.5653	440

Table - 2.B.6
X-ray diffraction data for $\text{Mg}_{0.5}\text{Cd}_{0.5}\text{Sm}_{0.5}\text{Fe}_{1.5}\text{O}_4$

Wavelength $\lambda = 1.5418 \text{ \AA}$

Lattice parameter $a = 8.6603 \text{ \AA}$

Structure = Cubic

Sr.No.	2θ deg.	$d_{\text{cal}} \text{ \AA}$	$d_{\text{obs}} \text{ \AA}$	(hkl)
1.	29.025	3.0001	3.0739	220
2.	35.045	2.5585	2.5585	311
3.	40.805	2.2096	2.2096	400
4.	53.325	1.7321	1.7166	422
5.	54.970	1.6330	1.6691	333
6.	58.910	1.5000	1.5665	440

Table 2.B.7

X-ray density (dx), physical density (da) and porosity % of ferrite samples, $Mg_x Cd_{1-x} Sm_y Fe_{2-y} O_4$ (x = 0.5)

Y	Composition	X-ray density dx gm/cm	Physical density da gm/cm	Porosity P %
0	$Mg_{0.5} Cd_{0.5} Sm_0 Fe_2 O_4$	5.021	4.1209	17.93
0.1	$Mg_{0.5} Cd_{0.5} Sm_{0.1} Fe_{1.9} O_4$	5.1997	3.6506	29.79
0.2	$Mg_{0.5} Cd_{0.5} Sm_{0.2} Fe_{1.8} O_4$	5.3565	2.6290	50.91
0.3	$Mg_{0.5} Cd_{0.5} Sm_{0.3} Fe_{1.7} O_4$	5.5828	3.6069	35.39
0.4	$Mg_{0.5} Cd_{0.5} Sm_{0.4} Fe_{1.6} O_4$	5.6161	3.9750	29.22
0.5	$Mg_{0.5} Cd_{0.5} Sm_{0.5} Fe_{1.5} O_4$	5.9569	2.8449	52.24

reflections in the X-ray diffraction pattern for spinel structures are (220), (311), (400), (422), (333), (440). It is further observed that for all the samples the observed and calculated d values agree well with each other. Close agreement between observed and calculated d values is an indicator that ferrites are fully formed with spinel structure. The results on samarium doped samples show that there is a little change in the lattice parameters of the parent samples. The small variation of lattice constant in case of undoped and doped samples may be due to variation in cation distribution or modification in the lattice.

The data on physical density (d_a), X-ray density (d_x) and porosity is given in Table 2.B.6. It can be seen from this table that both the physical density and X-ray density increases with increasing samarium content. The porosity however, shows a decreasing trend on addition of samarium.

Part - C

IR Studies

2.C.1 Introduction

IR spectroscopy can be used in the study of crystal chemistry of spinels. Prudhomme¹⁵ has distinguished three applications namely,

- i) determination of co-ordination of the cations in the spinel structure
- ii) study of cation ordering
- iii) study of the deformation of cubic spinel structure.

The distortion of cubic spinel structure is local one and limited to a few atomic distance or a co-operative one resulting in lowering the symmetry of the crystal structure. These distortions may be due to ionic ordering or originating from an electronic nature like Jahn Teller effect.

Two types of spectra are observed in the ferrites.

- i) Electronic spectra due to the electronic transitions and
- ii) Vibrational spectra due to the cation vibrations (Lattice vibrations of the oxide ions against the cations)

Infrared spectra of some on simple ferrites with the general formula MFe_2O_4 were examined by Waldron.¹⁶ For the analysis of spectra it is necessary to consider the vibrational spectrum of periodic structures. The vibrational problem is most conveniently treated by classification of crystals according to the continuity of bonding as (i) continuously bonded, (ii) discontinuously bonded and (iii) intermediate.

In continuously bonded crystals, the atoms are bonded to all nearest neighbours by equivalent forces (ionic, co-valent or Van der Walls) and the frequency distribution of vibrations is given by a Debye or Bervon Karman treatment of the classical

mechanical problem. In this class are included simple ionic crystals such as the alkali halides, diamond and its homologous, metals and rare gas crystals.

In the discontinuously bonded or molecular crystal, sets of atoms are tightly bonded by (intermolecular) chemical valence forces and separated from adjacent sets by weak (intermolecular) Van der Waals forces. In a first approximation the spectrum resembles that of a gas molecule with the vibrational lines slightly broadened due to weak intermolecular coupling. In addition there is a low frequency branch similar to the spectrum of a heavier rare-gas crystal. To this class belong the solid polyatomic gases, most organic compounds, sulphur and non-metallic compounds.

In the third class, the intermolecular forces are somewhat greater than those in the molecular case and the branches may overlap. The vibrational problem may occasionally be treated as a perturbation of the class 2 case. Examples of this group include ionic crystals containing polyatomic ions, hydrogen bonded crystals and strongly dipolar crystals.

Generally, ordering of cations results in a lowering of the overall symmetry which means an increasing number of IR active vibrations. So the infrared spectrum of the ordered spinels will show a fine structure compared with the disordered structure, but on the other hand, appearance of extra absorptions

in the spectra of solid solutions does not indicate any kind of ordering.¹⁷

A cursory inspection of the spectra shows two absorption bands below 1000 cm^{-1} appear as a common feature of all the ferrites. Absorption in this region is not restricted to this class of compounds but occurs in the spectra of most metallic oxides.¹⁸ The bands arise from lattice vibrations of the oxide ions against cations. At higher frequencies gradually increasing absorption caused by electronic transitions is observed.

Infrared studies on simple ferrites with the general formula $M\text{Fe}_2\text{O}_4$ was examined by Waldron. He has given the detailed analysis for computing force constant and specific heat of the material. He has also discussed modes of vibrations in spinels. Cubic or tetragonal distortion of manganese ferrites has been observed with IR spectra by Brabers. Most of the work was done by him to understand ionic ordering in Ti^{4+} containing spinels.^{19,20,21} V.R.K. Murthy et al.²² have studied the IR absorption in Ni-Zn ferrites. They have also considered that vibrations in band positions can be ascribed to change in the Fe-O bond distances in octahedral and tetrahedral sites. The vibration is similar to that observed by introducing foreign atoms in the spinel.²³

2.C.2 Experimental

The IR spectra of the ferrite samples were recorded at room temperature in the range 200 cm^{-1} to 800 cm^{-1} by using IR spectrometer (Perkin-Elmer model 783) in the KBr medium at USIC, Shivaji University, Kolhapur.

2.C.3 Results and Discussion

The Infrared absorption spectra for the samples $\text{Mg}_x\text{Cd}_{1-x}\text{Sm}_y\text{Fe}_{2-y}\text{O}_4$ ($x=0.5, y=0, 0.1, 0.2, 0.3, 0.4, 0.5$) are shown in figs. 2.C.1 to 2.C.6 respectively. Table 2.C.1 shows the wave numbers of different absorption bands in the samples.

In the spinel ferrites the vibrational frequencies depend upon cation mass, cation oxygen bonding distance and unit cell parameters. The present ferrite show two dominant absorption bands around 600 cm^{-1} and 425 cm^{-1} . The high frequency absorption band is designated as ν_1 while the low frequency absorption band is designated as ν_2 . Waldron²⁴ and Hafner²⁵, who were among the earliest to study the vibrational spectra of ferrites attributed the high frequency band ν_1 to the intrinsic

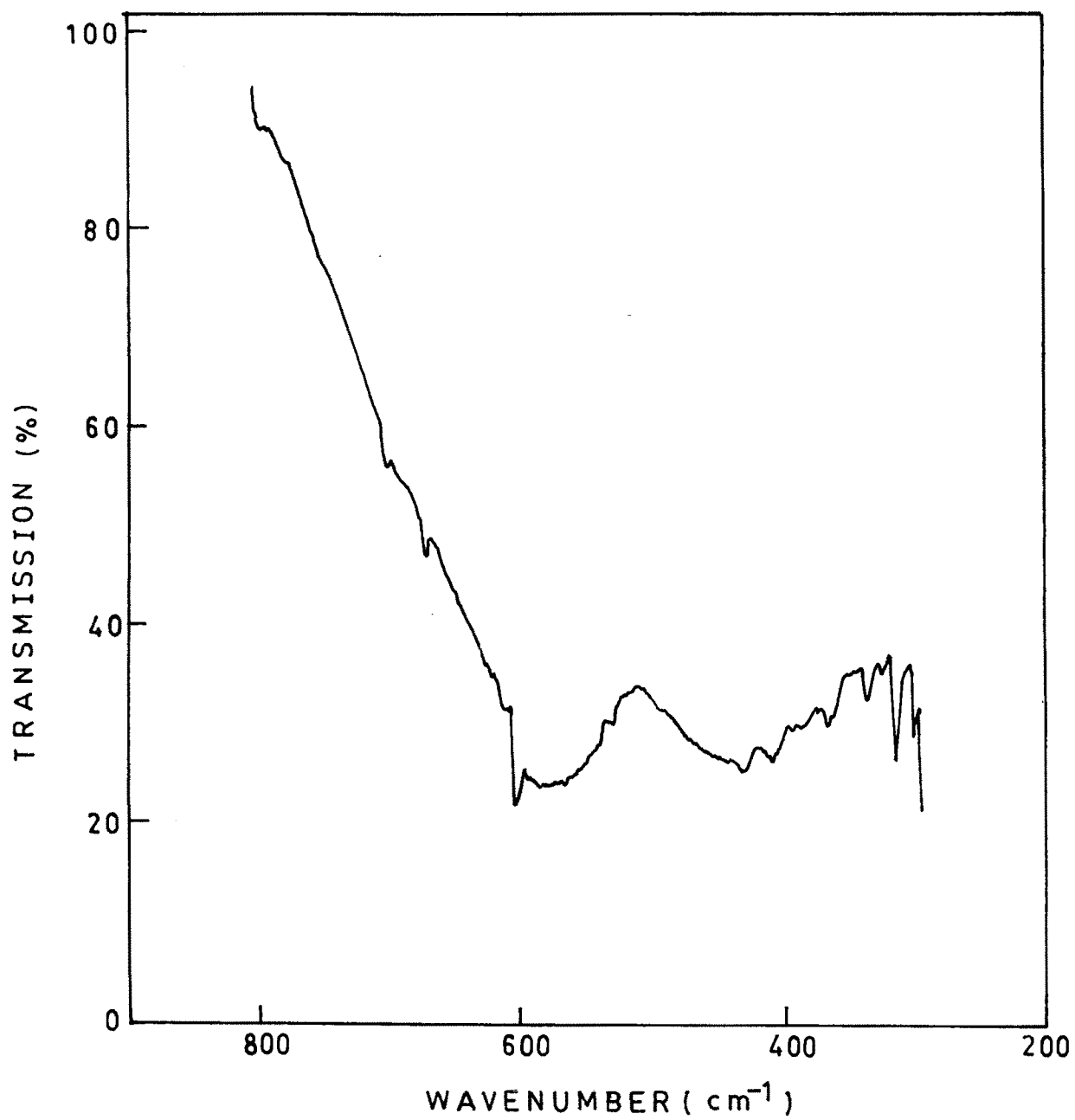
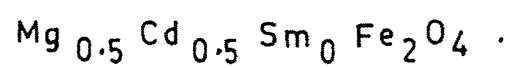


FIG. 2·C·1 - INFRARED ABSORPTION SPECTRUM OF



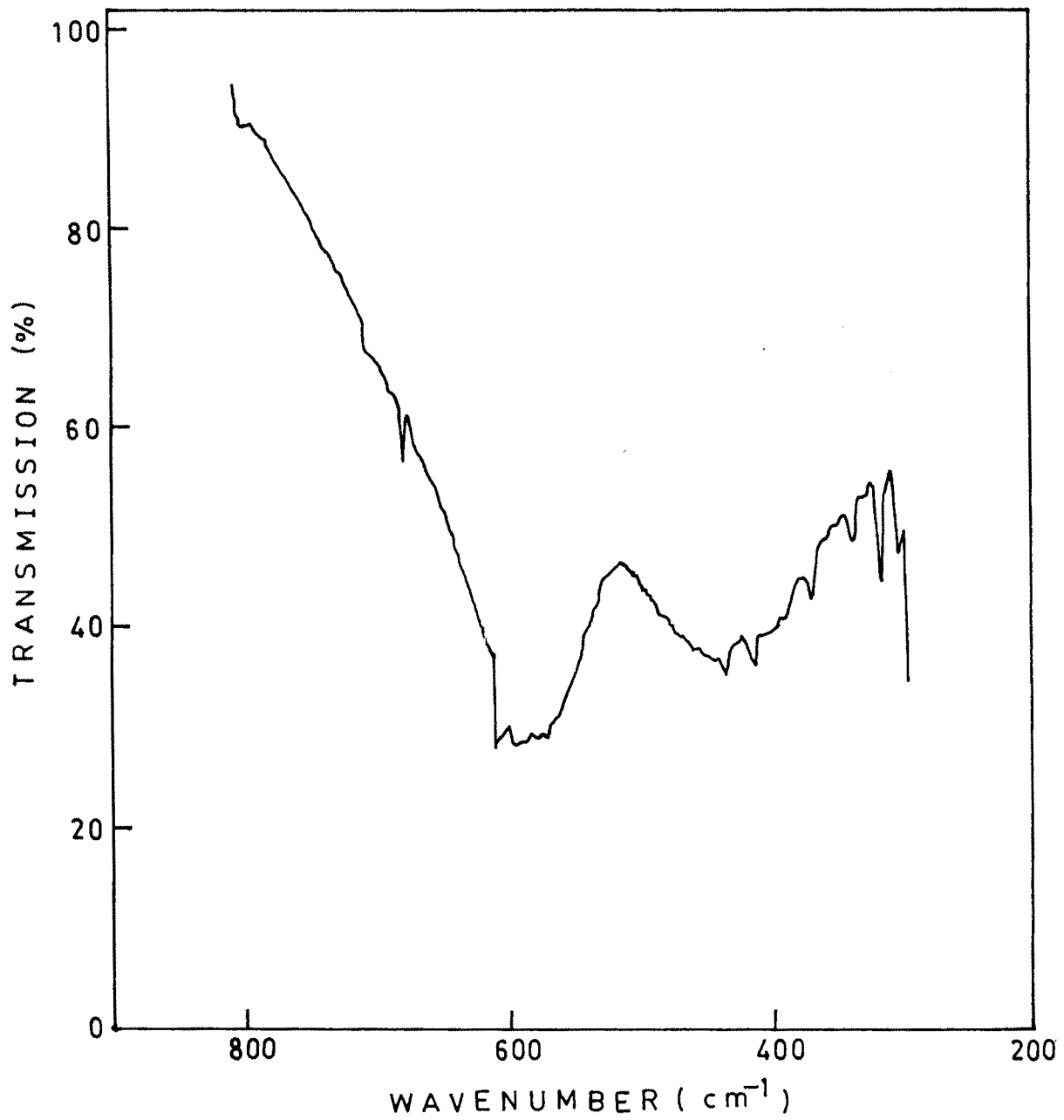
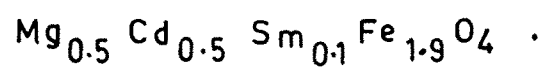


FIG. 2·C·2 — INFRARED ABSORPTION SPECTRUM OF



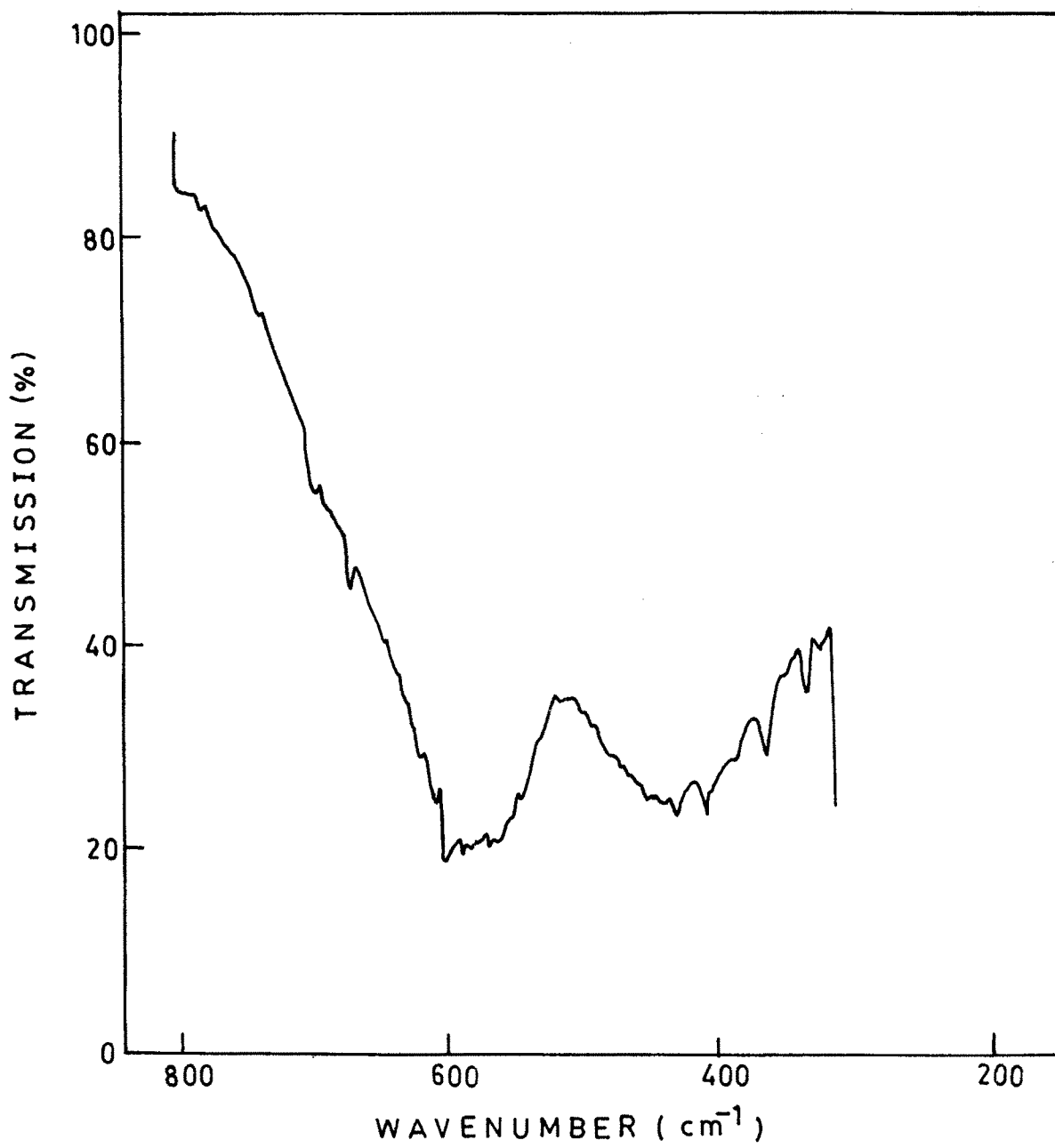
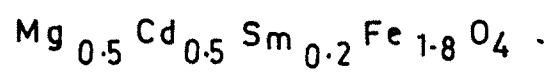


FIG. 2·C·3 - INFRARED ABSORPTION SPECTRUM OF



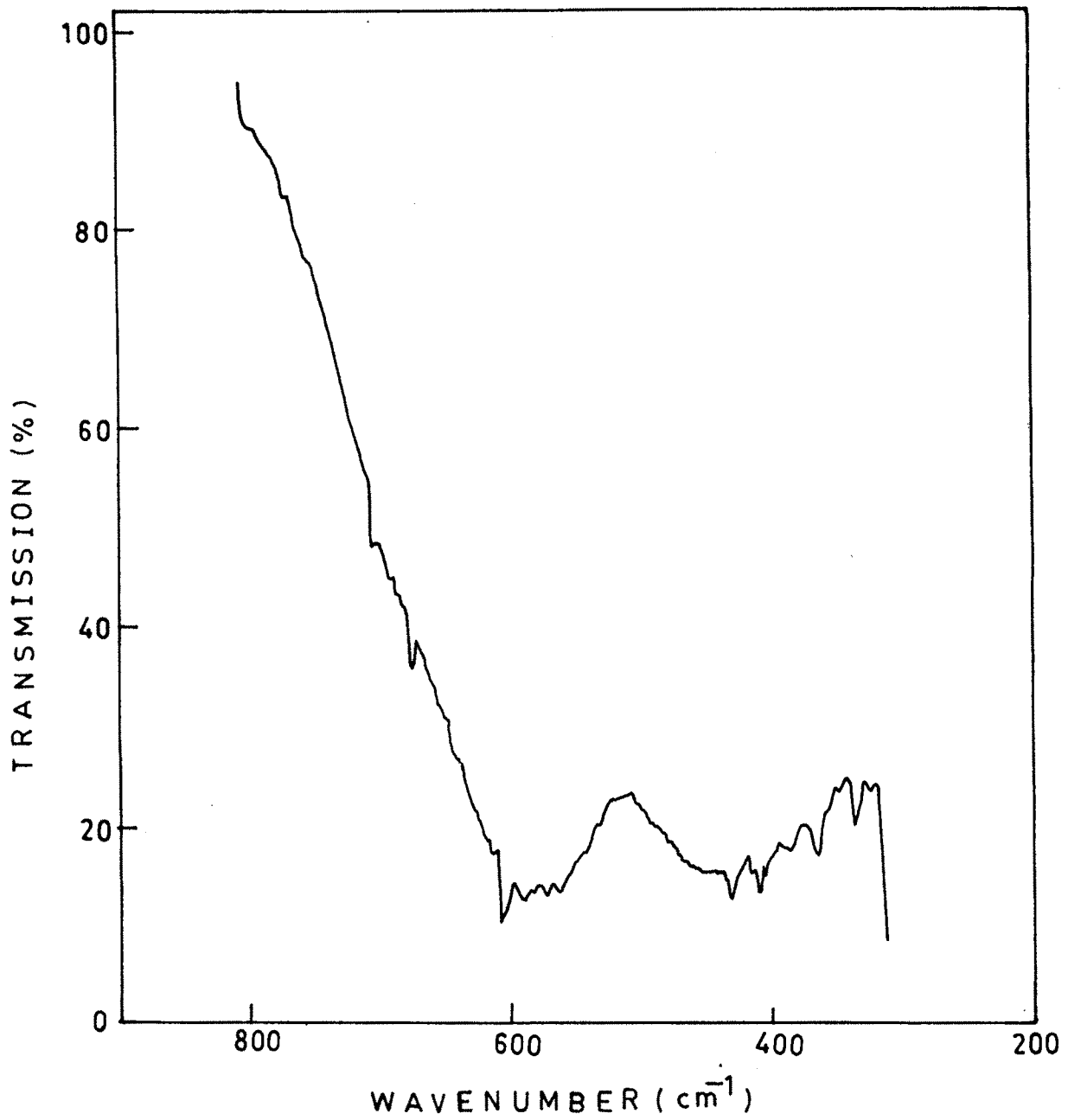
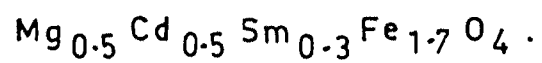


FIG. 2·C·4 - INFRARED ABSORPTION SPECTRUM OF



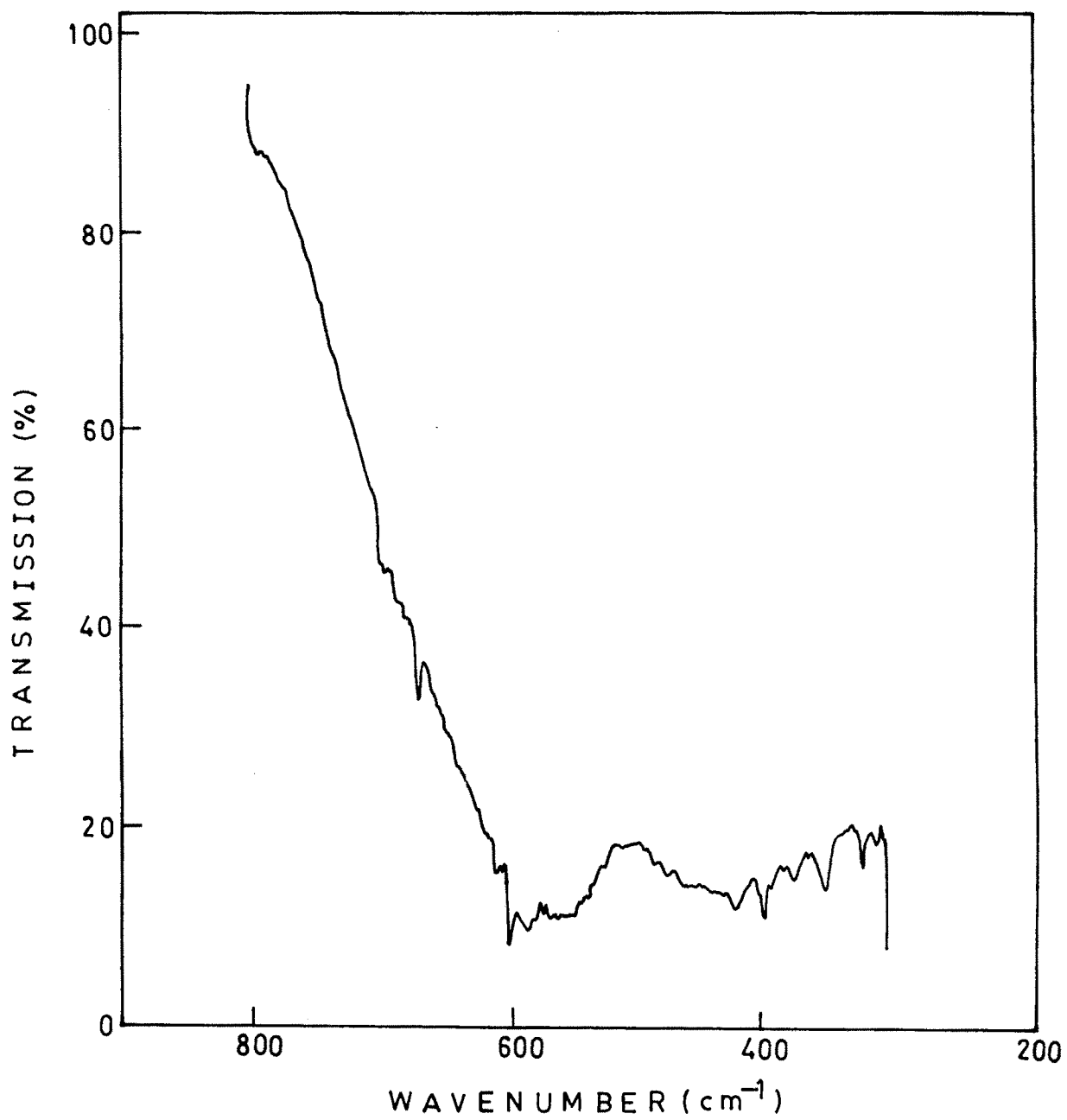
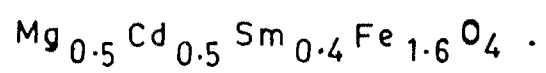


FIG. 2·C·5 - INFRARED ABSORPTION SPECTRUM OF



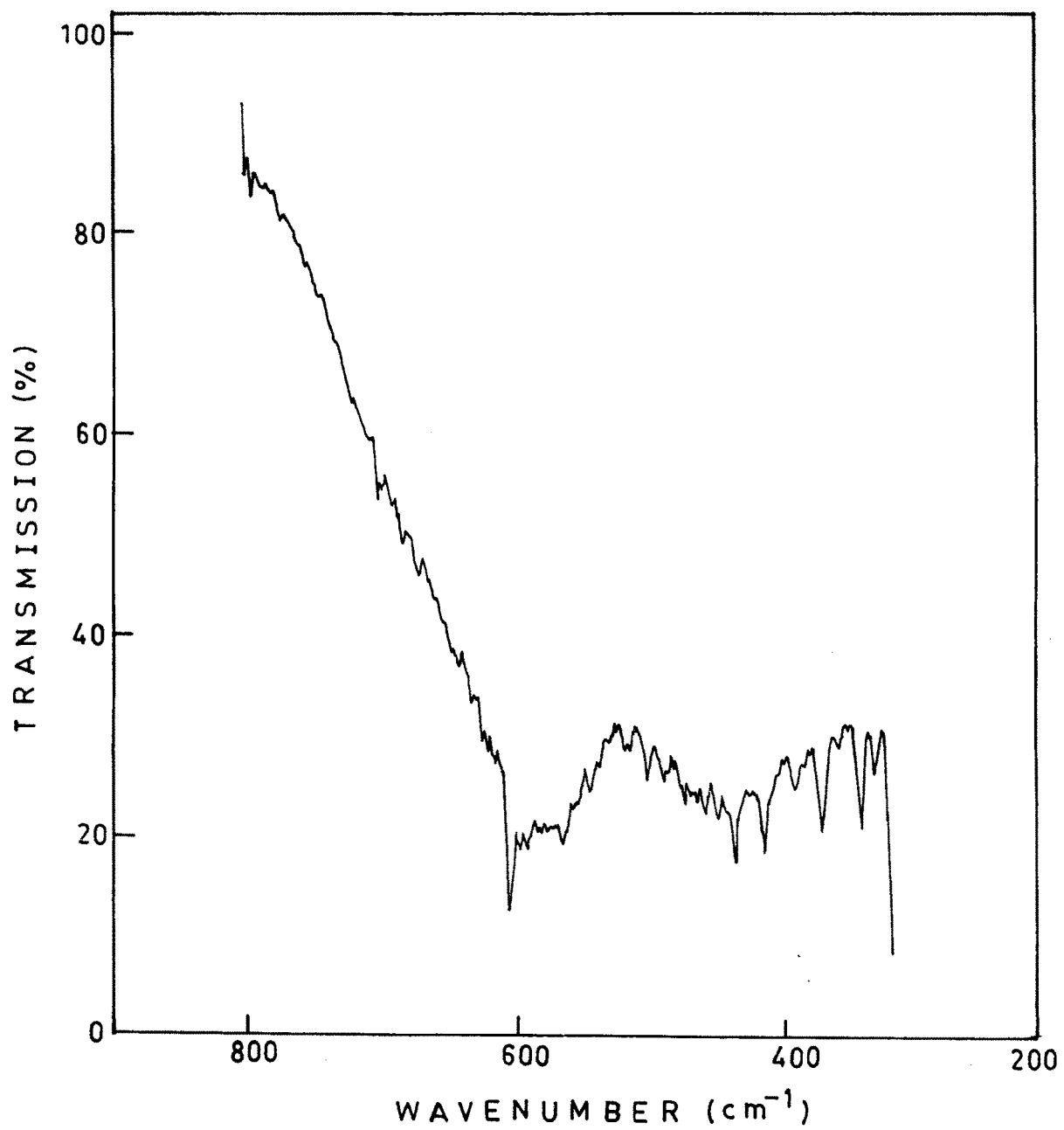


FIG. 2·C·6 — INFRARED ABSORPTION SPECTRUM OF
 $\text{Mg}_{0.5}\text{Cd}_{0.5}\text{Sm}_{0.5}\text{Fe}_{1.5}\text{O}_4$.

Table 2.C.1
Positions of IR absorption bonds in
 $Mg_x Cd_{1-x} Sm_y Fe_{2-y} O_4$ ferrites with $x = 0.5$

y	$\nu_1 \text{ cm}^{-1}$	$\nu_2 \text{ cm}^{-1}$	Composition
0	590	430	$Mg_{.5} Cd_{.5} Fe_2 O_4$
0.1	600	425	$Mg_{.5} Cd_{.5} Sm_{.1} Fe_{1.9} O_4$
0.2	590	425	$Mg_{.5} Cd_{.5} Sm_{.2} Fe_{1.8} O_4$
0.3	590	430	$Mg_{.5} Cd_{.5} Sm_{.3} Fe_{1.7} O_4$
0.4	580	400	$Mg_{.5} Cd_{.5} Sm_{.4} Fe_{1.6} O_4$
0.5	590	430	$Mg_{.5} Cd_{.5} Sm_{.5} Fe_{1.5} O_4$

Table 2.C.2
Bond length and force constant data for
 $Mg_x Cd_{1-x} Sm_y Fe_{2-y} O_4$ Ferrite with $X = 0.5$

Y	Composition	Bond lengths		Force constants dyne/cm	
		R_A (\AA)	R_B (\AA)	k_1	k_2
0	$Mg_{.5} Cd_{.5} Fe_2 O_4$	2.0248	2.0819	126195.55	263229.03
0.1	$Mg_{.5} Cd_{.5} Sm_{.1} Fe_{1.9} O_4$	2.0204	2.0774	123277.83	276953.58
0.2	$Mg_{.5} Cd_{.5} Sm_{.2} Fe_{1.8} O_4$	2.0230	2.078	123277.83	271325.31
0.3	$Mg_{.5} Cd_{.5} Sm_{.3} Fe_{1.7} O_4$	2.0277	2.0846	126195.55	274410.64
0.4	$Mg_{.5} Cd_{.5} Sm_{.4} Fe_{1.6} O_4$	2.0233	2.0804	109201.12	268481.75
0.5	$Mg_{.5} Cd_{.5} Sm_{.5} Fe_{1.5} O_4$	2.0424	2.1000	126195.55	279729.17

vibrations of the tetrahedral complexes and the band ν_2 to the octahedral complexes. Tarte et al.²⁶ observed that in normal ferrites both the absorption bands depend mainly on the nature of the octahedral cations and not much on the nature of the tetrahedral ions.

It has been noted earlier that the increase in band length normally leads to the decrease in the force constant. Shrivastava and Srinivasan²⁷ have, however, observed some unexpected results in the case of Ni-Cu ferrites. They have attributed this to the fact that oxygen can form, under favourable conditions, stronger bonds with metal ions even *at* longer internuclear separation. Similar behaviour has been observed for transition metal oxides with atomic numbers in the range $26 < Z < 29$ (28). Recently, Bhise et al.²⁸ have shown that force constants k_1 and k_2 increase with band lengths R_A and R_B . The results on the present series show that no such regular relation exists between bond lengths and force constants.

PART - D

Curie Temperature Measurements

2.D.1 Introduction

Curie temperature is a temperature at which a ferromagnetic or a ferrimagnetic state of a material changes to

paramagnetic state. It is also called a disordering temperature because the magnetic ordering is destroyed above this temperature. In the disordered state above the Curie temperature, thermal energy overrides any interaction between the local magnetic moments of ions. Below the Curie temperature, these interactions are predominant and force the local moments to order, so that there is a net spontaneous magnetization. Thus, Curie temperature (T_c) is the temperature below which there is a spontaneous magnetization (M) in the absence of an external applied magnetic field and above it the material is paramagnetic.

In the ferromagnetic case, as the temperature T increases from absolute zero, the spontaneous magnetization decreases from M_0 (the value of spontaneous magnetization at $T=0$) to zero. At first, this occurs gradually and then it increases rapidly until the magnetization disappears at the Curie temperature. In the ferrimagnetic materials the course of magnetization with temperature may be more complicated but the spontaneous magnetization disappears at the Curie temperature. In antiferromagnetic materials, the corresponding ordering temperature is termed as the Neel temperature. Below the Neel temperature, the magnetic sublattices have a spontaneous magnetization, though the net magnetization of the material is zero. Above the Neel temperature the material is paramagnetic.

2.D.2 Experimental

For the determination of Curie temperature by the Loroia technique, a soft iron rod of diameter less than the diameter of furnace was introduced into it from the upper end. The rod was magnetized by passing a current through a coil of copper wire. The pellet was stuck to the lower end of the magnet and it was heated.

The ferrite sample remained in contact with the electromagnet till the Curie temperature was attained. As soon as the Curie temperature was reached the ferrite sample lost its contact with the magnet and fell under gravity. The temperature at this moment was recorded with the help of thermocouple.

2.D.3 Results and Discussion

The Curie temperatures obtained by Loroia and permeability techniques as a function of samarium content are given in Table 2.D.1. It can be observed that the Curie temperature decreases continuously and linearly with increasing samarium content but it is very low when samarium is undoped. The observed decrease can be explained on the basis of exchange interaction between the ions. According to Neel's model the Curie temperature for a series of ferrites is proportional to the product of the iron (Fe^{3+}) contents on the two sites and their inter sublattice, $\text{Fe}_A\text{-O-Fe}_B$ distances and angles. In our system,

Table - 2.D.1

Values of Curie temperatures obtained by Loroia technique for
 $Mg_x Cd_{1-x} Sm_y Fe_{2-y} O_4$ system with $x = 0.5$

Y	Composition	Temperature °C
0	$Mg_{0.5} Cd_{0.5} Fe_2 O_4$	85
0.1	$Mg_{0.5} Cd_{0.5} Sm_{0.1} Fe_{1.9} O_4$	332
0.2	$Mg_{0.5} Cd_{0.5} Sm_{0.2} Fe_{1.8} O_4$	167
0.3	$Mg_{0.5} Cd_{0.5} Sm_{0.3} Fe_{1.7} O_4$	162
0.4	$Mg_{0.5} Cd_{0.5} Sm_{0.4} Fe_{1.6} O_4$	157
0.5	$Mg_{0.5} Cd_{0.5} Sm_{0.5} Fe_{1.5} O_4$	172

the substitution of Sm ions ($y=0, 0.1$ to 0.5) ions changes the iron ion concentration from 2 to $2-2y$ thereby decreasing the number of ferrous ions on the octahedral sites. Thus, the reduction of Tc can be related to the reduction in Fe^{3+} ions both on octahedral and tetrahedral sites on increasing of Sm concentration.

References :

1. K.J. Standley "Oxide Magnetic Materials" Chapter-2, p.9 Clearehdon Press, New York (1972).
2. Economus G. J. Amer. Ceram. Soc., 38, 241 (1955).
3. Robbin's H. "Ferrites" Proceedings of Third international conference on Ferrites, Kyoto, Japan (29 Sept.- 2nd Oct.1980).
4. Wolf W.P., IEEE Trans. Mag. 6, 795 (1970).
5. Sato T., IEEE Mag. 6, 795 (1970).
6. Sato T., Juroda C. and Saito M. "Ferrites" Proc. Int. Conference on ferrite" Kyoto, Japan p.72 (1970).
7. Lin-Bo Zhas IEEE Trans. Magn. (USA) vol. May 17 No.6 pp.3144-6 (Nov. 1981).
8. Wagner C. 2 Phys. Chem. B-34, 309-16 (1936).
9. Shull C.G., Wollan E.O. and Koenler W.C., Phys. Rev. 84 (1951) 912.
10. Hastings J.M. and Corliss L.M., Rev. Mod. Phys. 25 (1953) 114.
11. Prince E. and Treuting R.G., Acta. Cryst. 9(1956) 1025.
12. Bragg W.L., Nature (London) 95, 561 (1915).
13. Debye P. and Scherrer P., Physic 17, 277 (1916).
14. Hull A.N., Phy. Rev. 9, 84, 564 (1916) and ibid. 10, 661(1917).

15. Preudhomme J.C.R., Acad. Sci. (France) 267 C, 1632 (1968).
16. Waldron R.D., Phy. Rev. Vol.99 pp. 1727 (1955).
17. Preudhomme J. and Tarte P., Spectrochim Acta. 27A, 961 (1971), 27 A 845 (1971), 27A, 1817 (1971).
18. Harris L.J., Opt. Soc. America 45, 27 (1955).
19. Brabers V.A.M., Phys. Stat. Sol.(a) 12, 629 (1972).
20. Brabers V.A.M., Phys. Stat. Sol. 33, 563 (1969).
21. Brabers V.A.M., Phys. Stat. and Van denderghe R.E., Physics letters, Vol. 44A, 493 (1973).
22. Murthy V.R.K., Chitrashankar C., Reddy K.V. and Sobhanandri J., Indian Journal of pure and appl. Physics. Vol.16, 79-83 (1978).
23. Josyulu D.S. and Sobhandri J. Phys. Stat. Solidi. (a) 65, 479 (1981).
24. Waldron R.D., Phys. Rev. 99(6) (1955) 1727.
25. Hafner S.T., Z. Fur. Krist. 115 (1961) 331.
26. Tarte T., Spectrochimica Acta. 19 (1963) 49.
27. Srivastava C.M. and Srinivasan J.T., J. Appl. Phys. 53 (1982) 8148.
28. Herzberg G., "Molecular spectra and Molecular Structure" Vol.1 (1950).
29. Bhise B.V., Dongare M.B., Patil S.A. and Sawant S.R., J. Mater. Sci. Lett., 10 (1991) 922.
30. Loroia K.K. and Sinha A.P.B., Ind. J. Pure and Appl. Phys. 1 (1963) 215.